Blind Synchronization for NC-OFDM - When "Channels" Are Conventions, Not Mandates

Dola Saha[1], Aveek Dutta[2], Dirk Grunwald[1,2]and Douglas Sicker[1]
[1]Department of Computer Science
[2]Department of Electrical, Computer and Energy Engineering
University of Colorado
Boulder, CO 80309–0430 USA
Email: {Dola Saha, Aveek.Dutta, Dirk.Grunwald, Douglas.Sicker}@colorado.edu

***Abstract*—Recent efforts in making licensed spectrum available for secondary use have opened up new opportunities and has redefined the meaning of sharing spectrum. Sharing spectrum requires aggregation of multiple non-contiguous bands of varying width to communicate as a network. Rather than limiting spectrum access to fixed width narrowband channels, they should be treated as conventions that are highly flexible and allow for simultaneous multi-user communication among a variety of heterogeneous devices with different transceiver capabilities. Non-Contiguous Orthogonal Frequency Division Multiplexing (NC-OFDM) is a physical layer technique that can be utilized to achieve this goal. Unlike the contiguous channelized access model, wideband non-contiguous access posses a critical challenge of synchronization. In this paper, we propose a practical algorithm and hardware implementation to overcome this challenge. Equipped with this blind synchronizer, we propose a Medium Access Control (MAC) layer design to enable flexible channel access while achieving co-existence with the incumbent and other secondary heterogeneous networks. The blind synchronization technique vastly simplifies channel rendezvous in the secondary network and provides faster migration to a vacant spectrum. Through extensive simulations under varying signal-to-noise ratio (SNR) and spectral occupancy, we show significant improvement over existing algorithms employed for NC-OFDM synchronization in cognitive radios and make wideband cognitive radio networks a distinct possibility in the near future.**

I. Introduction

Bandwidth utilization in wireless communication not only refers to the range of radio frequencies used in a particular radio-wave transmission, but also to the duration of useful communication in the occupied bandwidth. Widespread spectrum measurements [1] and analysis [2] have shown the availability of *whitespaces* and enormous capacity that can be used by other users as long as they do not interfere with incumbents of that part of the spectrum. While shared usage of unused parts of licensed spectrum provides opportunity for higher bandwidth utilization, it also opens up a world of new challenges. Often these unused spectrum are available in *chunks* of frequency bands. The secondary user intending to use these chunks will have to transmit over non-adjacent frequencies while avoiding the frequencies used by the primary for that band. The term *Dynamic Spectrum Access (DSA)* has been coined to address the entire family of users that can handle such non-contiguous usage and the devices capable of DSA are termed *cognitive radios*. The cognitive radio not only needs to identify unused parts of the spectrum but also has to provide sustained communication over non-adjacent frequencies.

The availability of *whitespaces* in a cognitive radio network will vary over time with the duty cycle of the primary user. Every time this happens the communicating nodes will have to negotiate for the next set of available frequency bands. This negotiation is typically done by some form of message exchange using a dedicated radio channel, which is also shared by all the users in the network. Evidently, there is an intrinsic contention built into the system, where instead of contending for the communication channel nodes are contending for the control channel. Hence, the benefit of having DSA may be diminished by having a contention based control channel. Therefore, the goal of this paper is to provide in-band signalling for channel rendezvouz that is fast, simple and makes use of the reconfigurable radio. This paper proposes a mechanism of channel migration that is suited for future cognitive radio network employing DSA operating over a wide band of frequencies and that is pratical and implementable.

Current radios and spectrum allocation policy are tightly bound to the notion of "channels" that are, partly a historical part of spectrum allocation influenced by practical radio design of the time. The ability to operate over a wide radio spectrum may cause radio designs to look at the application characteristics of data streams when making PHY or MAC decisions. Factors such as power levels, achievable (or needed) modulation rates and the ability to trade total spectrum against each of these makes the decision of where and how to modulate more complex. Networks operating in a wide band need to know how to coordinate the stations within the network. This includes sensing when spectrum is no longer suitable for an application and deciding (and communicating) new resource allocations. Being able to modulate across a large spectrum allows communication to multiple stations simultaneously, but there are a number of PHY and MAC layer issues to resolve because some stations may use non-contiguous spectrum. In short, we envision a network of radio nodes that have one or more heterogeneous radio interfaces each able to flexibly construct signals to fill a radio band chosen from a wide range of bands. The goal is to rethink current radio network protocols to develop new protocols able to fully exploit these capabilities.

Just as different parts of the spectrum greatly influence the propagation of signals, the amount of spectrum used greatly impacts the bandwidth, the potential for interference and the MAC overhead. If different receivers are allocated their own spectrum, contention-based MAC overheads can effectively disappear. Likewise, the ability to allocate arbitrary spectrum amounts to individual flows or receivers means that capacity can be allocated at a much finer granularity than in traditional "channelized" MACs. Channelization is the most common approach to using the spectrum in the cognitive radio domain. However, the presence of a narrowband incumbent (say, a wireles microphone) might render an otherwise wideband channel unusable and lead to under utilization of the spectrum. At the same time, increased narrowing down of channels leads to multiple channels to which a device needs to tune to communicate. Restricted channelization limits the opportunistic exploitation of the spectrum when using a wideband radio. Hence, we propose a generalized concept of channel width that only depends on the bandwidth of the radio front ends on a communicating link and the available spectrum. Without this restriction, the AP can now decide on the optimum bandwidth and tuning frequency that can cater to a group of compatible devices using multiuser techniques like OFDMA, while avoiding the part of the spectrum occupied by an incumbent. The underlying data rate (or resistance to errors) can also be controlled by adjusting the OFDM parameters depending on the radio environment in which the links are communicating. This can be realized by employing distributed blind synchronization techniques for non-contiguous spectrum access as it eliminates any requirement of prior bandwidth negotiation: preliminary results of which are discussed in [3]. Thus, the MAC layer coordinates with the PHY to determine the spectrum management depending on the available spectrum, the radio environment, and the bandwidth requirement of participating clients to optimize the end-to-ends throughput.

Figure 1 shows an example of one such heterogeneous network, where the AP is communicating with the clients over different widths of non-contiguous spectrum. This secondary network coexists with a Primary transmission and another secondary network. We envision that the MAC, capable of communicating in this heterogeneous radio environment and achieving high end-to-end throughput will face several interrelated scheduling and allocation decisions. Clearly, using a wide 100-500MHz receiver allows a radio to transmit across a broader spectrum. In most heterodyne radio systems that use a "mixer" to modulate a carrier frequency, demodulation requires that the senders and receivers are on the same *center frequency* f_c. This constrains the selection of frequency bands used by different receivers unless it is possible to cause all receivers to "re-center" their center frequency. Rather than allocate purely contiguous spectrum to a single receiver, it may be more appropriate to use non-contiguous spectrum – this is made possible using the Non-Contiguous Orthogonal Frequency Division Multiplexing (NC-OFDM).

Co-existence of multiple users using the same carrier frequency has been little known until the evolution of multi-carrier communications technologies, like Orthogonal Frequency Division Multiplexing (OFDM) and their subsequent

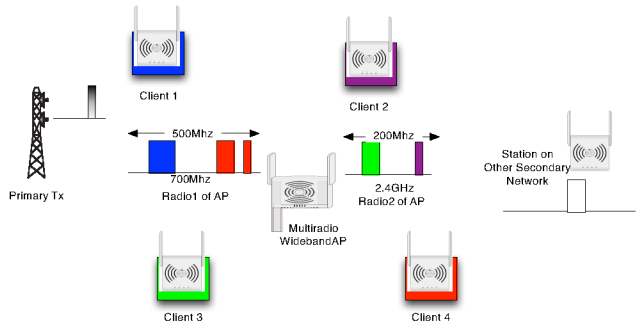

Fig. 1. Spectrum Sharing in Wideband Cognitive Radio Network: An example scenario. Secondary network, consisting of an AP and four clients, is coexisting in presence of primary and other secondary networks. The AP has two radios of different bandwidth, tuned to two different center frequencies, and is communicating over variable width NC-OFDM.

adoption for use in popular wireless protocols. Multi-carrier communication offers the advantage of enhanced spectrum utilization by slicing the bandwidth into closely packed, non-interfering data carriers. Once the bandwidth is available, information bits are placed in those data carriers and an inverse Fourier Transform produces one OFDM symbol of duration $N_{\text{fft}} \times F_s$ seconds (N_{fft} is the width of the Inverse Fourier Transform and F_s is the sampling frequency). At the receiver, a Fourier Transform of this symbol will reveal the information embedded in those data carriers. For the information to be retrieved with no or minimal error, the boundary of an OFDM symbol must be determined with high accuracy: the effect of mis-estimation is discussed in §III. This accuracy is ensured by the synchronizer in conjunction with other processing units like *packet detect* and *frequency offset correction.*

Synchronization is the process used to detect an incoming packet and also to identify the OFDM symbol boundaries with high accuracy. This is done by employing some form of time-domain correlation with a previously agreed upon sequence of bits or samples at the receiver. Since OFDM waveforms are modulated in frequency domain and then converted to time-domain signals, altering or notching some of the subcarriers as done in NC-OFDM will change the structure of the preamble. Unless otherwise notified, the receiver has no idea of this new sequence being used by the secondary transmitter. Hence, there must be a method the receiver can use to re-establish the correlation properties and ensure proper decoding of the signal and migrate to an empty part of the spectrum within a very short time.

In this research, we propose a distributed synchronization algorithm for NC-OFDM and its hardware implementation. We also present a MAC layer design that uses this synchronization technique to eliminate control channels for rendezvous and simplify channel allocation and network management in a wideband cognitive radio network.

Our Contributions: The key contributions of our research are as follows:

- We propose a distributed algorithm for blind (without prior knowledge of the transmitted frequencies) synchronization for preambles transmitted using NC-OFDM.

- In order to show that our algorithm can be implemented in realistic hardware, we present a programmable correlator structure that can be synthesized for FPGA.
- We analyzed the algorithm under a multi-path channel with varying SNR, yielding considerably better results at low SNR and low bandwidth occupancy compared to existing algorithms.
- Lastly, we propose a MAC framework that utilizes the synchronization technique to make wideband cognitive radio a reality by largely simplifying channel access and its control.

II. Related Work

In this section we discuss prior work that motivated our research and how the proposed algorithm and design compare with similar research in this field. As already addressed, distributed synchronization is critical for NC-OFDM based cognitive radio communication. Blind estimation of OFDM parameters has been studied in detail. Authors in [4], [5] discuss Cyclic Prefix(CP) based autocorrelation algorithms to extract symbol timing. However, these methods work for contiguous OFDM transmission as they rely on estimating the sampling frequency, and in turn the FFT/IFFT size. This method is good for coarse symbol timing but does not guarantee a good time-domain correlation for fine timing information. In [6], authors present a theoretical approach to NC-OFDM synchronization. The main drawback of a CP based correlation is that the correlation energy depends greatly on the CP length, number of non-contiguous subchannels used and the number of subcarriers used to encode the signal. In a true cognitive radio these parameters can vary over a wide range, further degrading the quality of the correlation.

Apart from cyclic prefix, embedded cyclostationarity features in the signal have been used to extract symbol timing as discussed in [7]. Unlike conventional OFDM, this method requires the modulation of multiple subcarriers with the same information to create the cyclostationarity feature in the signal. This requires more bandwidth than what would be used in conventional NC-OFDM. Feng et. al. proposes preamble design using sequences with superior autocorrelation property in [8]. However, it requires high spectral occupancy for successful correlation.

Implementations of NC-OFDM based cognitive radio waveforms have been shown using GnuRadio in [9], which assumes that the receiver has the knowledge of the non-contiguous spectrum used by the secondary transmission, which may not be possible in a true cognitive radio communication. Nolan et. al. in [10], provide an analysis of the preamble based synchronization using NC-OFDM. They have defined bounds on the minimum number of subcarriers required to be able to detect a packet. But this method performs the time-domain correlation with a known preamble that occupies the entire spectrum. This results in degraded correlation when spectrum usage is small.

Platforms like KUAR [11], WARP [12] and SORA [13] are some examples of well-known hardware platforms that support NC-OFDM transmission. These platforms either use some form of back-end central synchronization or use a predefined set of correlation co-efficients to detect the signal. In contrast to these, our work presents a completely distributed and blind synchronization method suited for cognitive radio networks.

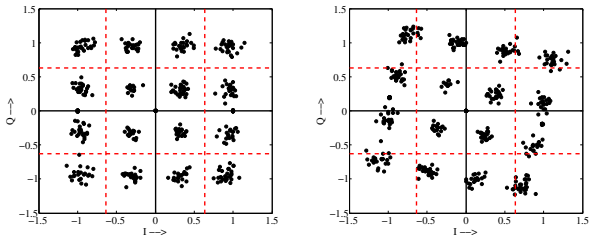

(a) Without Timing Offset (b) With Timing Offset

Fig. 2. Effect of symbol timing offset: 16QAM constellation after equalization at SNR = 15.5 with multi-path fading and a timing offset of (-8) samples. The decoding regions are shown by the red dotted lines.

Existing literature on cognitive radio has focused on control over a relatively small section of the radio spectrum. Often, this has involved methods such as dynamically allocating spectrum blocks [14], [15] or adaptive channel widths [16], [17]. Both the schemes employ a dedicated control channel and handshaking based protocol to agree on the spectrum and the median time to re-negotiate channel is of the order of tens of miliseconds, whereas [8] use a dedicated set of OFDM subcarriers to exhange control messages, which in turn limits the usable bandwidth. Compared to these, our mechanism can migrate to a diffrent part of the spectrum within few nanoseconds, which we discuss in the following sections. Similarly the 802.22 [18], CogNea [19] or ECMA 392 standardization efforts cover the use of a single spectrum region (the TV white spaces), and often focus on narrow-band channels of $6MHz$. These efforts address important problems – the coordinated use of a (relatively) large block of underutilized spectrum in the face of incumbents. But these efforts do not take advantage of the full range of available spectrum by limiting the access of the medium to a *mandated* channelized model, rather than using them as mere *conventions* that adapt based on a changing demand and resource availability for which we need fast in-band synchronization algorithms.

Thus, the lack of a proper distributed synchronization algorithm over non-contiguous bands has largely impaired the implementation of wideband cognitive radio. With the techniques and design discussed in this paper we intend to open new avenues toward making wideband cognitive radio networks a reality.

III. OFDM Symbol Timing

OFDM is a frequency domain modulation technique where the fidelity of the information is highly dependent on the frequency domain properties of the signal, like power spectral density and phase-magnitude variation across the signal bandwidth. OFDM symbols are generated by inverse Fourier Transform on blocks of data to preserve orthogonality between the subcarriers. Multiple blocks are concatenated in time to

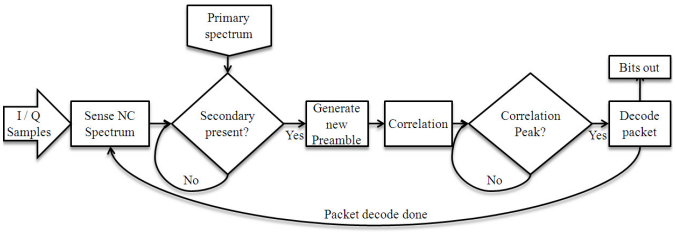

Fig. 3. NC-OFDM Synchronization Pipeline

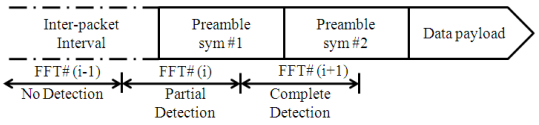

Fig. 4. Spectrum Detection

form a packet. Often the orthogonality is damaged due to multi-path effects of the channel and also by other receiver impairments like incorrect sampling frequency and I/Q offset during down conversion. The block type generation of OFDM calls for a similar decoding method at the receiver to recover the frequency domain modulations. Offset in symbol timing introduces phase noise in the subcarriers and affects phase modulations like BPSK and QPSK. The effect of phase noise has been examined in great detail in previous work [20], [21], [22]. In its simple form, failure to identify the correct symbol boundary results in phase rotation proportional to the number of samples offset from the correct boundary. Figure 2 shows an example of the effect of timing offset on demodulation. Figure 2(a) is a 16QAM equalized constellation transmitted using a 64 subcarrier OFDM, which has no timing offset. The correct timing ensures that there is no phase noise in the I/Q constellation, and using the red-dotted lines showing the decoding boundaries the bits can be extracted without errors. In contrast, figure 2(b) shows the equalized constellation, except the signal block is now offset by 8 samples. Significant phase rotation is seen, which causes the constellation points to cross the decoding boundaries leading to undesired errors. However, there is an allowable offset that will vary based on the amount of the allowable degradation for the constellation, e.g., for BPSK, theoretically, we can allow a rotation of $\pi/2$, although the consequence of such enormous offsets on other processing units are to be considered. Therefore, we can emperically derive that for a low to medium SNR an offset of less than 3 samples can be set as a benchmark for error-free decoding of a non-contiguous OFDM waveform. This benchmark can only be met by an accurate synchronizer in the time-domain which minimizes the average timing offset for an OFDM symbol over a wide range of occupied bandwidth and SNR. A primary transmission will also add interference to a secondary trasmission and alter the time domain representation of the preamble used by the secondary nodes. Therefore, we have to consider the effects of primary and secondary occupancies and their corresponding SNR at the secondary receiver. We discuss the synchronization technique in the following section, and discuss performance in §VI under realistic channel conditions.

IV. NC-OFDM Synchronizer

Synchronization is performed using a known sequence that is transmitted over multiple OFDM symbols at the beginning of every packet, aptly named the preamble. A correlator is used to compute the similarity of the incoming sequence of noisy samples to a locally stored copy of the preamble. The uniqueness of the preamble ensures superior correlation at the receiver, which is in turn used to identify the OFDM symbol boundary. Now, when using non-contiguous spectrum, the secondary fails to use the pre-defined preamble, which occupies a wider, and most importantly contiguous band of frequency than what is currently available. While encoding data over non-contiguous bands is easily achieved, synchronizing at the receiver poses a challenge. A receiver, trying to correlate with the pre-defined preamble will fail since the non-contiguous encoding of the signal has changed the time-domain representation of the preamble. This requires the receiver of a cognitive radio signal to be able to adapt to the changing environment. In contrast to the conventional synchronizer, the unit must be intelligent to be able to identify the data carriers used for the preamble, as well as change the parameters of the time-domain correlator to search for the correct OFDM symbol boundary.

This blind NC-OFDM synchronization is done in two steps:

- **Subcarrier Detection:** Since the receiver has no knowledge of the frequencies used by the cognitive transmitter, it has to detect the subcarriers present in the incoming signal by employing spectrum sensing across the entire band. It is assumed that the secondary nodes willing to share the licensed spectrum will have prior knowledge of the location, signal structure and power of the primary. This is a very realistic assumption if the secondary network uses database look-up to identify whitespaces, which has also been adopted as a part of recent spectrum sharing mandates by the FCC [23].
- **Regenerate Preamble and Correlate:** Once the data carriers are detected, a new preamble is generated locally at the receiver using the detected datacarriers only and the correlator is reprogrammed with the new co-efficients corresponding the samples of this preamble. In this way, we can ensure that whatever the incoming sequence is, we can re-establish the correlation based synchronization with high accuracy.

A. Spectrum Detection

Since the objective is to perform blind synchronization, i.e., with prior knowledge of the secondary spectrum, a secondary receiver must gather the subcarriers present in the incoming signal. Figure 3 shows the receiver pipeline for blind synchronization. Spectrum is sensed by computing FFT on the incoming I/Q samples, and the SNR for each subcarrier is measured. These results are compared to a threshold to decide on the presence of a subcarrier in the signal. This is followed by a decision making process to ascertain the exact width of each non-contiguous band of the secondary, as well as the primary that co-exist in time with the secondary. Figure 4

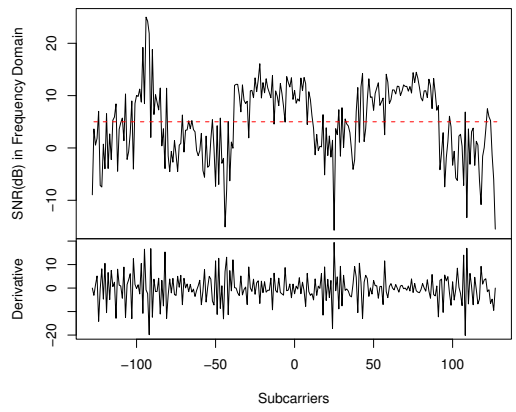

Fig. 5. NC-OFDM Waveform - Primary occupancy is subcarriers $[-95 : -91]$ and for secondary it is $[-38 : 11], [40 : 89]$.

shows a typical packet structure and the corresponding FFT windows. A secondary receiver begins spectrum sensing during the *inter-packet duration* denoted by FFT(i-1). As time progresses, the packet will start to appear in the FFT window as denoted by FFT(i). Depending on the number of samples of the packet that is present in the FFT window, the energy of the OFDM subcarriers will vary. In the subsequent FFT window, FFT(i+1), we see that signal is completely contained within the FFT window, hence providing an *estimate* of the spectrum. This *estimate* is further processed and strengthened by the decision engine that follows the FFT, and together they form the detection engine. As seen in Figure 4, using two preamble symbols at the beginning of the packet will ensure successful detection of the spectrum. Since the synchronization process works as a pipeline, it only stalls when the correlation detects an incoming packet with sufficient accuracy. Therefore, depending on when the signal arrives at the receiver, we can either get good correlation from the sensing results in the i^{th} FFT window or the $(i+1)^{th}$ window.

Decision Engine: Figure 5 shows an example spectrum detection using a threshold test that is empirically derived for a particular receiver and channel setting. The spectrum of the wave reveals the subcarrier occupancy of the narrowband primary and the non-contiguous secondary transmission. The spectrum is normalized so that the average noise floor is maintained at $0dB$ so that the threshold can be independent of any fluctuations of the noise floor. This is done by measuring the noise floor during the inter-packet duration using conventional MAC "quiet times" and subtracting it from the FFT output. From the threshold test we extract a "binary mask" of width equal to the number of FFT bins in which the *ones* denote the presence of a subcarrier and *zeros* denote the absence. The mask derived from the input signal contains the primary and secondary transmissions. With prior knowledge of the primary transmission, a *XOR* operation will extract the mask of the secondary transmission only.

When signals from independent sources overlap in time and are received over a multi-path channel, it affects the orthogonality of the OFDM subcarriers and results in inter-carrier interference leading to spurious unwanted fading at the band edges, frequency selective notching within a band and attenuation. In order to make the detection robust and practical, we employ some rules to handle these spurious anomalies in the detection and correct the "binary mask" to accurately represent the secondary:

Rule 1: Remove Outliers –If two or less spurious subcarriers are detected with no carriers on either side - they are deleted from the mask.

Rule 2: Fill Notches – If two or less nulls are detected in the mask with at least two carriers on either side, then fill those notches as they are considered part of a valid secondary band.

Rule 3: Identify Channel Bounds – Left edge is denoted by five consecutive nulls followed by five consecutive carriers and right edge by five consecutive ones followed by five consecutive zeros, given an inter-band guard distance of at least 10 carriers and minimum 5 carriers required to be considered as a valid secondary band.

Rule 4: Adjust Band Boundaries – Secondary bands are designed to begin at multiples of five. Therefore, the final mask can be either broadened or squeezed, so that the start is a multiple of five.

Once these corrections are made to the mask, the band detection, and consequently the synchronization, is greatly improved and ensures proper decoding of the packet. We discuss these results in §VI and §VII.

As an alternative to thresholding on instantaneous spectrum measurement, edge detection by thresholding on the first order derivative has been discussed in [9]. However, it is not suitable for instantaneous detection of spectrum by performing a single FFT on the signal, as shown in figure 5, and would require prolonged averaging often in the order of tens of OFDM symbols that incurs additional latency in packet detection, which is not optimal in most cases. In comparison, the method proposed here requires only two OFDM symbols and coupled with logic to correct for spurious measurements, make this technique very effective for cognitive radio networks.

B. Re-generate Preamble

The detection logic is followed by the actual correlation and subsequent synchronization. The mask computed at the detection stage is used to regenerate the time-domain preamble locally at the receiver. Using the frequency domain representation of a preamble, we select the indices corresponding to the *ones* in the mask while nulling out the other subcarriers as shown in figure 3. This results in an accurate estimation of the preamble that is used by the transmitter. Once the time-domain samples of the preamble are regenerated by an Inverse Fourier Transform, the correlator coefficients are initialized with these samples. After initialization, the correlation energy is computed using a buffered version of the incoming packet to include all time samples from the begining of packet. Once the correlation is successful, the packet decoding is initiated. During this time the spectrum sensing sensing results are disregarded.

C. Update Correlation Coefficients

If the correlation fails to satisfy a pre-defined threshold, then the spectrum sensing unit which operates in pipeline mode,

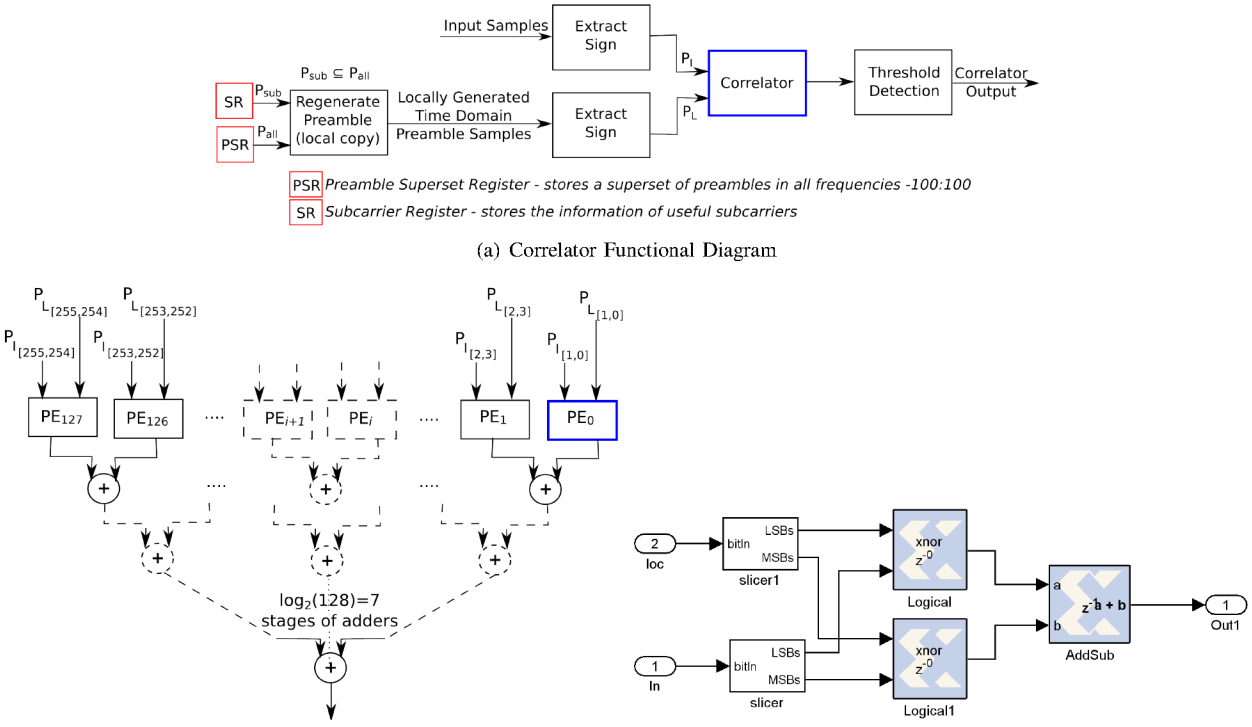

(a) Correlator Functional Diagram

(b) Correlator Inner Structure

(c) Smallest Processing Engine

Fig. 6. FPGA Implementation of a Programmable Correlator

will provide the detection unit with a new spectral measurement every N_{FFT}(FFT size) samples and the correlator is updated with the new mask again to test for the preamble of the next packet. Failure to detect a packet using a threshold can happen when the secondary signal SNR, relative to the primary, is very low and the secondary signal is overwhelmed by the high power primary. Under these circumstances we employ a simple re-transmission based protocol and also increase the guard band between the primary and secondary. We can re-establish the threshold based detection and correlation by this method and the results are discussed in §VII. However, we find that under normal operating range of SNR and spectral occupancy, the threshold test is able to determine the correct spectrum over a wide range. This is discussed in section §VI.

V. FPGA Implementation

In order to show that the synchronization algorithm is also suitable for hardware implementation, we propose a lightweight correlator structure that augments an existing OFDM based synchronizer and can be implemented in a FPGA. We base our programmable correlator on designs mentioned in prior works [24], [25], which implements synchronizers in hardware for contiguous OFDM. Figure 6(a) shows the structure of a programmable correlation unit that implements the proposed synchronization algorithm. The components of the correlator are as follows:

Acquire Spectrum Information: Spectrum sensing is an integral part of cognitive radios. Depending on the design choice, the spectrum sensing unit can be implemented as a part of the radio processing engine or as a separate unit that is a part of a cognitive engine. In either case, the correlator should have good co-ordination with this unit. The spectrum sensing unit provides the correlator and other key baseband processing units, like the equalizer and demodulator, with the information about the subcarriers used in a particular packet. Therefore, a programmable interface is required between the sensing unit and the baseband processing pipeline. Figure 6(a) shows a set of programmable registers that can be accessed by the spectrum sensing unit to update the "binary" mask from the detection unit for the most recent sensing results. The *Subcarrier Register(SR)* holds the mask to be used for regenerating the preamble in the following step.

Regenerate Preamble: Regenerating the preamble is required to establish the time-domain correlation. Usually for a particular network, the complete frequency domain preamble is pre-defined, and spans over all the subcarriers. Since cognitive radio can operate in multiple networks, this preamble can change. In hardware, we define a *Preamble Superset Register (PSR)* that holds the complete frequency domain preamble for the current network. Using the subcarrier map from the *SR* register and the preamble superset from the *PSR* register, the time-domain preamble is regenerated using inverse Fourier Transform. This preamble is used to perform the correlation with the incoming packet to extract the symbol timing.

Correlator Core: A time-domain correlator employs a running comparison of the input I/Q samples with a local copy of the time-domain samples of the preamble being searched for. The basic operation in a correlator is multiply-accumulate-shift for every fixed-point complex sample entering the correlator. Therefore, depending on the number of samples to be matched,

TABLE I
NC-OFDM PARAMETERS

Parameter	Value/Range
FFT size (N_{fft})	256 sample
Cyclic Prefix size	64 sample
Sampling frequency (f_s)	$80MHz$
Subcarrier spacing (f_s/N_{fft})	$312.5KHz$
Preamble superset	802.16 [26]
Number of preamble symbols	2 [27]
Subcarriers per band - Secondary	$10-100$
Subcarriers per band - Primary	$18-72$ (simulates a $6Mhz$ TV band)
Guard subcarriers	10

the size of the correlator and the number of gates to implement the logic in FPGA increases as it requires more number of adders, multipliers and shift registers. To make the correlator easily implementable, instead of performing wide (14 to 16 bits) fixed-point multiplications we use the *sign bit* of the input I/Q samples and the locally regenerated preamble samples. In doing so, the comparison of two samples reduces to a simple *XNOR* logic operation. Whenever the sign of the input sample matches with that of the local copy, the output is a '1', otherwise '0'. Constructing a tree of 2-input adders we can accumulate the result of the comparison for every shift operation within one clock cycle. Figure 6(b) shows the adder tree of the correlator for a 256 sample correlator. For a complex input, similar structure is repeated for the I and the Q paths. Figure 6(c) shows the *XNOR* processing engine designed using Xilinx System Generator, which performs comparison on two samples. Although the Correlator uses 1 bit instead of the usual 16 bits, we still find the performance to be satisfactory under varying SNR. We discuss the performance of the correlator and its resource consumption in §VI.

VI. RESULTS AND IMPLEMENTATION

In this section, the proposed synchronization method is evaluated by simulations in Matlab under varying channel conditions (SNR) and spectrum occupancy. The objective is to show the performance of the synchronization and subcarrier detection as a function of the primary and secondary parameters. The signal structure and the simulation environment are shown in table I. The channel used in the experiment is derived using a standard channel model built in Matlab (the *stdchan* function), along with additive white Gaussian noise. The chosen multi-path model has a 6 path delay profile for a $802.11a/g$ network. The frequency response and path delay of the channel is shown in Figure 7. Since the system (OFDM parameters) is designed on top of a $802.11a/g$ transceiver, so is the channel model chosen to evaluate it. Lastly, each experiment has been repeated for 500 iterations to average out jitters in the results.

While evaluating the algorithm we have identified a set of parameters that could vary in a network. Two of these parameters are varied at every analysis to limit the data set to three dimensions and for ease of presentation. Unless otherwise mentioned in the plots, the default values of the parameters are used for the analysis as given in table II. The metric that has been used throughout the analysis is the mean absolute error in samples about the correct symbol boundary

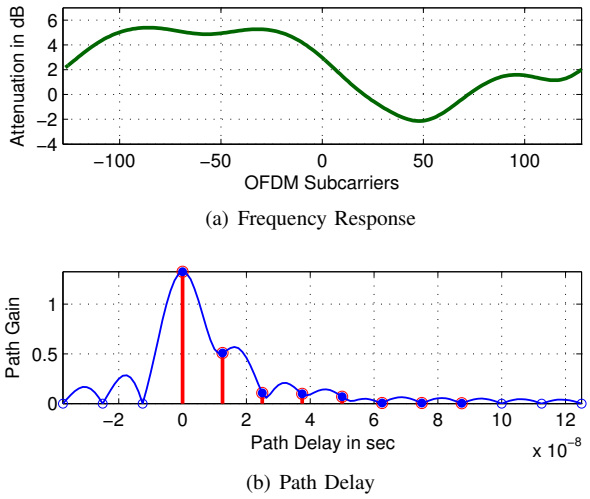

(a) Frequency Response

(b) Path Delay

Fig. 7. Multi-path Channel Response

TABLE II
DEFAULT SETTING FOR SIMULATION PARAMETERS

Parameter	Default Value
Primary SNR (SNR_p)	15 dB
Secondary SNR (SNR_s)	15 dB
Number of primary bands ($NBand_p$)	1
Subcarriers per band - primary (NSC_p)	18
Number of secondary bands ($NBand_s$)	1
Subcarriers per band - secondary (NSC_s)	20

and a benchmark of less than 3 has been set for proper decoding of bits from a symbol.

A. Comparison with cyclic prefix based correlation

NC-OFDM Symbol timing using cyclic prefix (CP) is one of the methods found in the literature and the proposed technique is compared with it to measure the improvement. It has been shown that the CP-based algorithm provides a coarse estimation of symbol timing [22] and this coarse timing estimate leads to phase noise and erroneous decoding of the signal constellation. In figure 8(a), the error is measured with varying secondary spectrum occupancy, i.e., varying the number of subcarriers per band, as well as varying the number of used by the secondary. Since CP-based timing relies heavily on the length of the cyclic prefix, and also on the similarity of the cyclic prefix to the OFDM symbol, the correlation energy is severely degraded for smaller CP length and lower numbers of non-contiguous subcarriers. Our method shows an improvement of more than $20-30$ times over cyclic prefix correlation. Most importantly the mean error is below 1. Figure 8(b) shows the error magnitude with varying secondary SNR and number of bands. Mean error is maintained fairly constant at ≤ 1 sample across varying SNR, whereas the CP-based correlation varies from $10-50$ samples.

B. Varying primary SNR

The next set of results show the performance of the technique when the primary SNR is varied. Figure 9(a) shows that when the relative SNR of the secondary is higher than

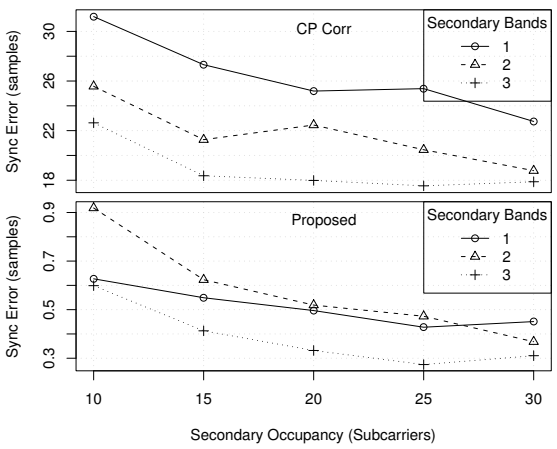

(a) Increasing Secondary Occupancy

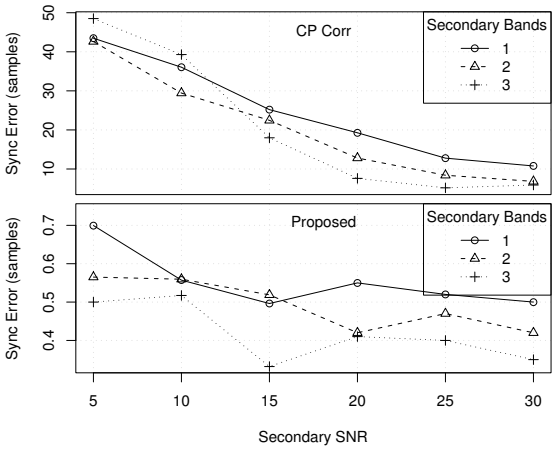

(b) Increasing Secondary SNR

Fig. 8. Comparison with CP-based Correlation

that of the primary, the average error is maintained below 1 sample. Only when the primary tends to overwhelm the secondary transmission the error is greater. It is to be noted that when the primary signal is stronger than the secondary by more than $20dB$, it represents a very hostile situation for secondary operation and can be considered as the worst possible case. Figure 9(b) shows that when the secondary SNR is held constant, the error decreases with an increase in the number of secondary spectral bands (because correlation is performed across more subcarriers). Similarly, with the number of secondary bands remaining constant, the error decreases with an increase in the bandwidth of the secondary (*i.e.* more subcarriers) as shown in figure 9(c). In all the cases, the worst case performance is ≤ 2 samples of synchronization error.

C. Varying primary occupancy

As the width of the primary signal increases it tends to produce inter-carrier interference and starts to bleed into adjacent carriers, which could potentially be a secondary band. Figure 10(a) and 10(c) shows reduction in average error with increase in secondary SNR and occupancy, respectively. This trend is also seen with an increasing number of secondary bands in figure 10(b) as the number of secondary subcarriers involved in correlation is more.

D. Varying number of primary bands

In this experiment the effect of multiple primary links in the network on secondary links is studied. In figure 11(a), the error magnitude is measured by varying the primary SNR. Understandably, when 3 independent primary links are present the correlation performs worst at low secodary SNR. In contrast, when secondary occupancy increases or more number of disjoint bands are used then the correlation improves as shown in figure 11(b). The trend continues in figure 11(c) where a wider secondary band gives the best performance while a narrow band secondary is subdued by multiple primary links.

An interesting observation from these experiments is that the synchronization performs well even with errors in estimating the secondary band edges. This is primarily attributed to the good correlation properties of the preamble chosen for these experiments. Hence, the quality of synchronization not only depends on the secondary subcarriers, it also depends on the cross-correlation properties of the preamble. In order to achieve correct band-edge detection in multi-path fading channels, we propose a channel sounding and re-transmission technique in §VII which, in conjunction with the preamble properties, make this approach practical for cognitive radio network. The experiments and the results discussed herein, provide a key insight into the trade-offs that can be exploited, while deploying cognitive radio networks. It is the wise selection of transmission parameters that spans across multiple dimensions of SNR, band width and number of non-contiguous subcarriers that will provide the optimum performance in a network. We acknowledge that this problem requires further research and this paper is a positive step towards setting the foundation for such future work.

E. Hardware Implementation

We have implemented a prototype correlator in FPGA and tested it with a simulated channel, due to the unavailability of a wideband front-end. Figure 12 shows the input and output traces of the correlator for a NC-OFDM waveform. In figure 12(a), the input spectrum occupies subcarriers $[-68 : -17]$ and subcarriers $[44 : 69]$. The spectrum detection unit detects this and programs the correlator registers with the spectral mask to regenerate the preamble. The *sign* bit and *XNOR* based correlator output is shown in figure 12(b). Since we have used two preamble symbols to synchronize, we get two distinct peaks that are detected using a simple threshold test. These encouraging results motivate us to perform over-the-air experiments using wideband front-ends, which we leave as a future extension of this work. The design has been synthesized for a Virtex-IV FPGA, and the utilization is given in table III, which includes preamble regeneration using an

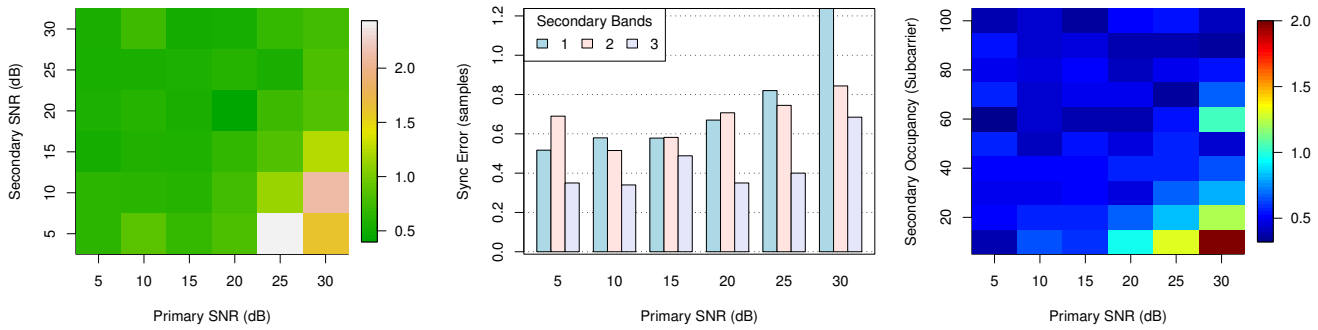

(a) SNR_p vs SNR_s (b) SNR_p vs $NBand_s$ (c) SNR_p vs NSC_s

Fig. 9. Average Synchronization Error (in Samples) with Increasing Primary SNR

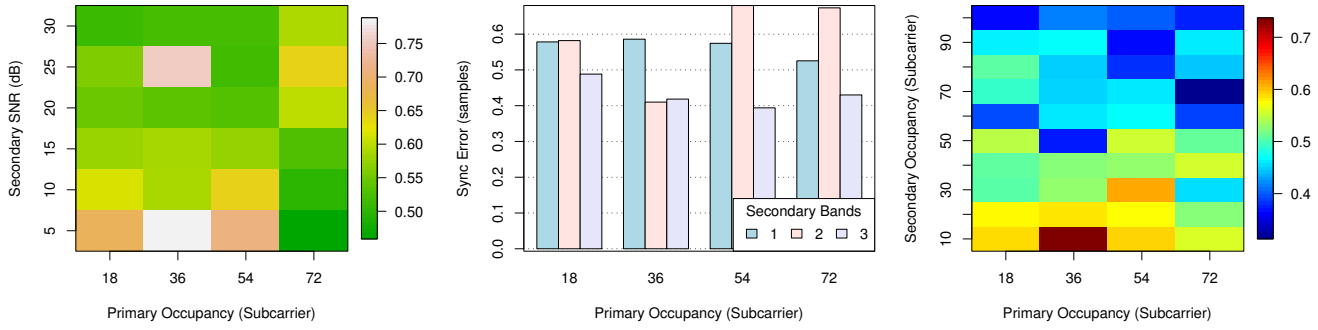

(a) NSC_p vs SNR_s (b) NSC_p vs $NBand_s$ (c) NSC_p vs NSC_s

Fig. 10. Average Synchronization Error (in Samples) with Increasing Primary Occupancy

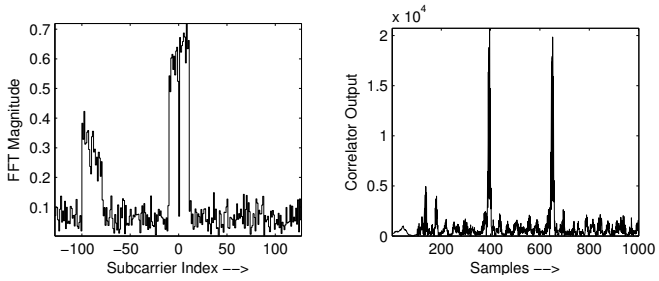

(a) Non-Contiguous Spectrum (b) Correlator output

Fig. 12. Programmable Correlator Input and Output

TABLE III
NC-OFDM CORRELATOR UTILIZATION IN VIRTEX - IV

Parameter	Count / Max	Utilization
Slices	2900/15360	18.80%
Slice Flip Flops	1950/30720	6.35%
4 input LUTs	3309/30720	10.77%
FIFO16/RAMB16s	4/192	2.08%

IFFT core. The correlator design and implementation is a step toward designing realistic cognitive radio hardware and we are actively working in implementing other transceiver components to work as a wideband cognitive radio using NC-OFDM.

VII. ROBUST SUBCARRIER DETECTION

The control channel can be eliminated when blind synchronization is followed by error-free packet decoding. To decode a packet, transmitted over NC-OFDM subcarriers, it is necessary to detect the frequency domain properties of the signal correctly, such that information bits can be extracted from the correct set of modulated subcarriers. In this section, we discuss a MAC layer protocol to ensure correct detection of the subcarriers using the techniques presented in §IV.

A. Observations and Insights

Figure 13 shows an example FFT spectrum, with one primary band and the secondary is transmitting in three non-contiguous bands. When the primary and the secondary transmissions have comparable SNR, as in figure 13(a), the secondary subcarriers can be detected correctly without any error using threshold test. Figure 13(b) shows a worst case scenario, where the measured SNR in the primary band is $\approx 20dB$ higher compared to that of the secondary bands or 100 times stronger. It is observed that a) the power of primary signal bleeds in the other parts of the spectrum and increases the average noise floor, b) frequency selective fading from two multi-path channels causes one of the secondary bands to undergo high attenuation and cannot be detected. c)

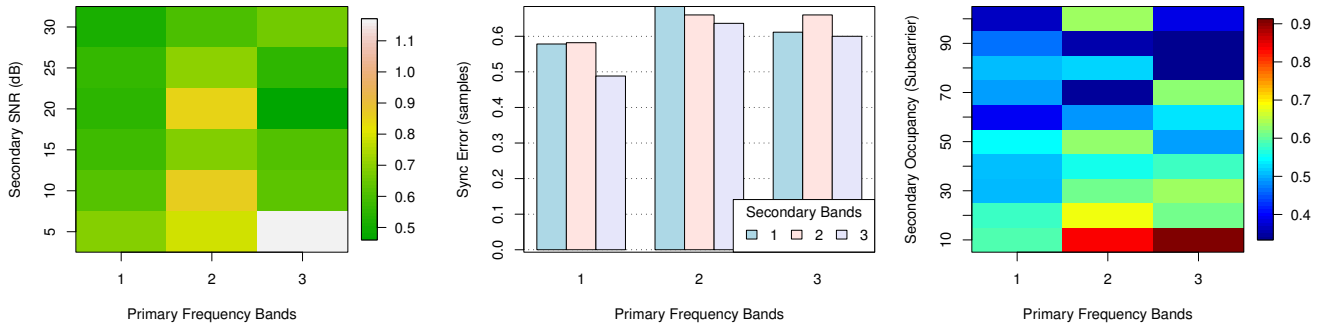

(a) $NBand_p$ vs SNR_s (b) $NBand_p$ vs $NBand_s$ (c) $NBand_p$ vs NSC_s

Fig. 11. Average Synchronization Error (in Samples) with Increasing Primary Bands

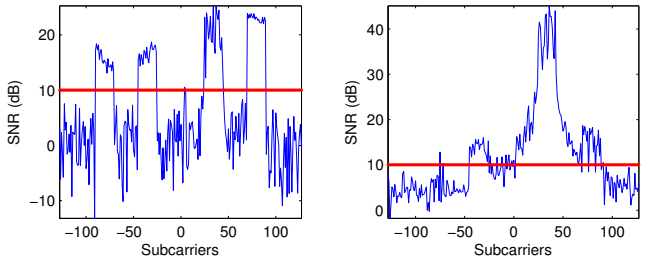

(a) Comparable Power Primary (b) High Power Primary

Fig. 13. NC-OFDM Transmission of Secondary ($[-90 : -71], [-45 : -26], [70 : 89]$) in Presence of Primary ($[25 : 42]$)

whereas, the same threshold can be used to detect the other two secondary bands.

Since the noise floor gets elevated in the presence of a strong primary signal, higher signal power is required to maintain the SNR requirement to decode the secondary signal. Alternatively, we can design a stopband filter to suppress the high power unwanted signal. Filter design for OFDM application is difficult because the phase response of the filter for OFDM has to be linear and deterministic so it can be compensated by equalization later. Also, the amplitude response should have a sharp cut-off within the guard-band between two non-contiguous bands. We recognize that the filter design is a separate piece of research which we intend to pursue as future work and is out of scope of this work. Depending on the relative difference in the SNRs the guard band will vary and this choice can be negotiated between the secondary nodes to maximize the utilization of the spectrum.

B. Subcarrier Detection by Retransmission

In the presence of frequency selective fading the transceiver pair should avoid communicating in that part of the spectrum within the channel coherence time. To address this issue the communicating nodes participate in a simple *channel sounding* mechanism, where the transmitter retransmits using a randomly chosen subset of last used set of subbands: only this time it uses $(N-1)$ bands instead of N. Since the other two bands can be correctly detected using the synchronization techniques in §IV, connection can be reestablished between the transceiver pair. This selective channel fading information can be used to modulate variable datarates [28] at different subcarriers to maximally utilize the band.

We perform experiments to show the detection capability of our proposed protocol in varying primary and secondary conditions. Figure 14 shows the percentage of correct spectrum detection (only the transmitted subcarriers are detected) without retransmission and with one retransmission. In all the cases, multiple secondary bands lead to lower detection percentage due to the frequency selective fading. Hence, during re-connection it is beneficial to use narrower single band than multiple bands. Figures 14(a) and 14(b) show the detection percentage with increasing primary and secondary occupancies respectively. We do not notice much variation in detection percentage with increasing primary occupancy, which indicates that our system remains unaffected with increasing primary subcarriers. With increasing secondary occupancy, the percentage of successful detection reduces, because more subcarriers are prone to channel fading. Using an increased number of sub bands also results in worse performance because detecting "an edge" is important, and an increased number of sub bands also means an increased number of edges.

Using one retransmission yields a detection percentage of $> 90\%$ in most of the cases. Figures 14(c) and 14(d) show the performance of the detection system with varying primary and secondary SNRs respectively. We notice that at high primary SNR and at low secondary SNR, where the relative difference is $\geq 20dB$, the primary overwhelms the secondary signal, and the need to employ filters and variable guard band is very much evident which will help to improve the results, as discussed in §VII-A. In other combination of SNR and spectrum occupancy, a retransmission yields a detection percentage of $> 90\%$.

When comparing this method to the use of a control channel, it's important to recognize that a dedicated control channel can experience frequency selective fading and unwanted signals or interference In such cases, our method provides greater flexibility in choosing non-contiguous chunks of spectrum for retransmission. Also, in a stable network the dedicated frequency set for control channel remains unutilized

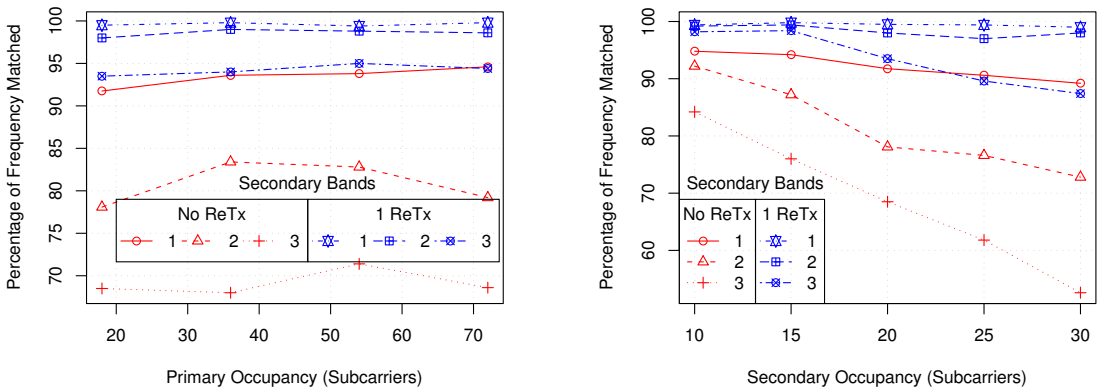

(a) Increasing Primary Subcarrier

(b) Increasing Secondary Subcarrier

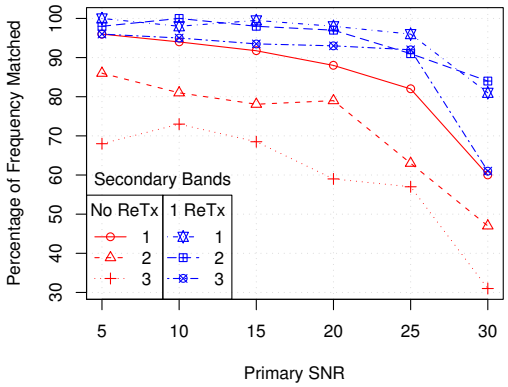

(c) Increasing Primary SNR

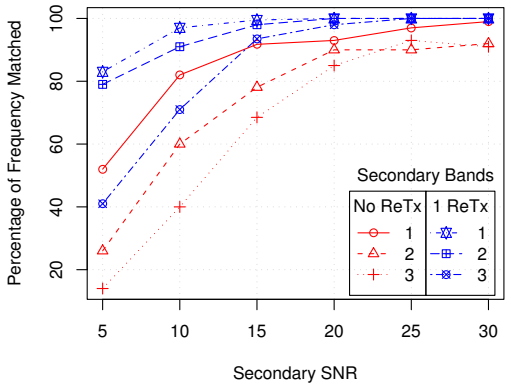

(d) Increasing Secondary SNR

Fig. 14. Secondary Band Detection (All Subcarriers in a Band) With and Without Retransmission

while in this technique we can use for useful communication. We believe that these results can further be improved by the use of proper filtering techniques which is not considered here. Failure to decode a packet correctly might trigger the secondary receiver to transmit tones [29] in the subcarriers in which it detected the packet. This will help the transmitter to know which parts of the spectrum are fading. This information can be used at the transmitter end to suppress the fading parts of the spectrum during retransmission.

VIII. Future Work

The focus of this research is primarily on evaluation of a novel technique for fine synchronization of NC-OFDM packets and ensure error-free decoding of a complete packet. As a part future work, we are actively involved in designing and building a wideband ($\geq 100MHz$) cognitive radio network testbed including the hardware and the algorithms required for it to function in a dynamic spectrum. We also intend to introduce digital filtering techniques to enhance the quality of secondary receptions and finally test the system in white spaces available in the TV band.

IX. Acknowledgment

This work is being funded by NSF/GENI Project 1803, "CR-GENI - Cognitive Radios for Geni". Portions of the work were also funded by the NSF award 0627172 "NeTS-FIND: Radio Wormholes for Wireless Label Switched Mesh Networks" and equipment support from award 0454404 "CRI: Wireless Internet Building Blocks for Research, Policy, and Education".

X. Conclusion

In this paper we have proposed a set of techniques that can make NC-OFDM transmissions more practical by addressing the synchronization challenges involved. Simple detection technique coupled with programmable radio hardware can lead to fast channel rendezvous between secondary nodes without the requirement of a dedicated control channel. We have also validated our approach using realistic simulations that shows the synchronization technique outperforms existing solutions by order of magnitude and is robust against changing channel conditions. While much work remains to be done, this research shows a new approach towards solving one of the most challenging problems in deploying cognitive radio networks.

References

[1] "Spectrum Occupancy Measurements : http://www.sharedspectrum.com/measurements/." [Online]. Available: http://www.sharedspectrum.com/measurements/

[2] K. Harrison, S. Mishra, and A. Sahai, "How much white-space capacity is there?" in *New Frontiers in Dynamic Spectrum, 2010 IEEE Symposium on*, apr. 2010, pp. 1 –10.

[3] A. Dutta, D. Saha, D. Grunwald, and D. Sicker, "Practial implementation of blind sychronization in NC-OFDM based cognitive radio networks," in *Proceedings of the Workshop on Cognitive Radio Networks (CoRoNet'10)*, Sept 2010.

[4] M. Shi, Y. Bar-Ness, and W. Su, "Blind ofdm systems parameters estimation for software defined radio," in *New Frontiers in Dynamic Spectrum Access Networks, 2007. DySPAN 2007. 2nd IEEE International Symposium on*, 17-20 2007, pp. 119 –122.

[5] H. Ishii and G. Wornell, "Ofdm blind parameter identification in cognitive radios," in *Personal, Indoor and Mobile Radio Communications, 2005. PIMRC 2005. IEEE 16th International Symposium on*, vol. 1, 11-14 2005, pp. 700 –705.

[6] J. Acharya, H. Viswanathan, and S. Venkatesan, "Timing acquisition for non contiguous ofdm based dynamic spectrum access," *New Frontiers in Dynamic Spectrum Access Networks, 2008. DySPAN 2008. 3rd IEEE Symposium on*, pp. 1–10, Oct. 2008.

[7] P. Sutton, B. Ozgul, K. Nolan, and L. Doyle, "Bandwidth-adaptive waveforms for dynamic spectrum access networks," in *New Frontiers in Dynamic Spectrum Access Networks, 2008. DySPAN 2008. 3rd IEEE Symposium on*, 14-17 2008, pp. 1 –7.

[8] S. Feng, H. Zheng, H. Wang, J. Liu, and P. Zhang, "Preamble design for non-contiguous spectrum usage in cognitive radio networks," in *WCNC'09: Proceedings of the 2009 IEEE conference on Wireless Communications & Networking Conference*. Piscataway, NJ, USA: IEEE Press, 2009, pp. 705–710.

[9] L. Yang, W. Hou, L. Cao, B. Y. Zhao, and H. Zheng, "Supporting demanding wireless applications with frequency-agile radios," in *Proc. of ACM/USENIX NSDI*, San Jose, CA, April 2010.

[10] K. E. Nolan, T. W. Rondeau, P. Sutton, and L. E. Doyle, "Tests and trials of software-defined and cognitive radio in ireland," in *SDR Forum Technical Conference and Product Exposition*, 2007.

[11] R. Rajbanshi, A. M. Wyglinski, and G. J. Minden, "An efficient implementation of nc-ofdm transceivers for cognitive radios," in *in Proc. of 1st Conf. on Cognitive Radio Oriented Wireless Networks and Commun., Mykonos*, 2006.

[12] P. Murphy, A. Sabharwal, and B. Aazhang, "Design of warp: A flexible wireless open-access research platform," in *Proceedings of EUSIPCO*, 2006.

[13] K. Tan, J. Zhang, J. Fang, H. Liu, Y. Ye, S. Wang, Y. Zhang, H. Wu, W. Wang, and G. M. Voelker, "Sora: high performance software radio using general purpose multi-core processors," in *NSDI'09: Proceedings of the 6th USENIX symposium on Networked systems design and implementation*. Berkeley, CA, USA: USENIX Association, 2009, pp. 75–90.

[14] P. Bahl, R. Chandra, T. Moscibroda, R. Murty, and M. Welsh, "White space networking with wi-fi like connectivity," *SIGCOMM Comput. Commun. Rev.*, vol. 39, no. 4, pp. 27–38, 2009.

[15] Y. Yuan, P. Bahl, R. Chandra, P. Chou, J. Ferrell, T. Moscibroda, S. Narlanka, and Y. Wu, "Knows: Cognitive radio networks over white spaces," apr. 2007, pp. 416 –427.

[16] R. Chandra, R. Mahajan, T. Moscibroda, R. Raghavendra, and P. Bahl, "A case for adapting channel width in wireless networks," *SIGCOMM Comput. Commun. Rev.*, vol. 38, no. 4, pp. 135–146, 2008.

[17] Y. Yuan, P. Bahl, R. Chandra, T. Moscibroda, and Y. Wu, "Allocating dynamic time-spectrum blocks in cognitive radio networks," in *Proceedings of the 8th ACM international symposium on Mobile ad hoc networking and computing*, ser. MobiHoc '07. New York, NY, USA: ACM, 2007, pp. 130–139. [Online]. Available: http://doi.acm.org/10.1145/1288107.1288125

[18] *IEEE 802 LAN/MAN Standards Committee 802.22 Working Group on WRANs*, IEEE Computer Society : LAN/MAN Standards Committee. [Online]. Available: http://www.ieee802.org/22/

[19] J. Wang, M. S. Song, S. Santhiveeran, K. Lim, G. Ko, K. Kim, S. H. Hwang, M. Ghosh, V. Gaddam, and K. Challapali, "First cognitive radio networking standard for personal/portable devices in tv white spaces," in *New Frontiers in Dynamic Spectrum, 2010 IEEE Symposium on*, apr. 2010, pp. 1 –12.

[20] M. Speth, S. Fechtel, G. Fock, and H. Meyr, "Optimum receiver design for wireless broad-band systems using OFDM - I," in *Communications, IEEE Transactions on*, vol. 47, Nov 1999, pp. 1668–1677.

[21] ——, "Optimum receiver design for OFDM-based broadband transmission - II. A case study," in *Communications, IEEE Transactions on*, vol. 49, Apr 2001, pp. 571–578.

[22] T. Chiueh and T. P, *Chapter : Synchronization*. John Wiley and Sons (Asia) Pte. Ltd., 2007.

[23] *FCC Ruling on Unlicensed operation in TV whitespaces*, Federal Communication Commission. [Online]. Available: http://www.fcc.gov/Daily_Releases/Daily_Business/2010/db1025/FCC-10-174A1.pdf

[24] A. Dutta, J. Fifield, G. Schelle, D. Grunwald, and D. Sicker, "An intelligent physical layer for cognitive radio networks," in *WICON 2008: Proceedings of the Fourth International Wireless Internet Conference (WICON 2008)*. New York, NY, USA: ACM, 2008.

[25] A. Troya, K. Maharatna, M. Krstic, E. Grass, and R. Kraemer, "Ofdm synchronizer implementation for an ieee 802.11(a) compliant modem," in *IASTED International Conference on Wireless and Optical Communication, 2002*. IASTED, 2002, pp. 152–157. [Online]. Available: http://eprints.ecs.soton.ac.uk/13552/

[26] *Part 16: Air Interface for Fixed and Mobile Broadband Wireless Access Systems*, IEEE Computer Society : LAN/MAN Standards Committee. [Online]. Available: http://standards.ieee.org/getieee802/download/802.11-2007.pdf

[27] *Part 11: Wireless LAN Medium Access Control (MAC) and Physical Layer (PHY) Specifications*, IEEE Computer Society : LAN/MAN Standards Committee. [Online]. Available: http://standards.ieee.org/getieee802/802.11.html

[28] H. Rahul, F. Edalat, D. Katabi, and C. G. Sodini, "Frequency-aware rate adaptation and mac protocols," in *Proceedings of the 15th annual international conference on Mobile computing and networking*, ser. MobiCom '09. New York, NY, USA: ACM, 2009, pp. 193–204. [Online]. Available: http://doi.acm.org/10.1145/1614320.1614342

[29] A. Dutta, D. Saha, D. Grunwald, and D. Sicker, "Smack: a smart acknowledgment scheme for broadcast messages in wireless networks," *SIGCOMM Comput. Commun. Rev.*, vol. 39, no. 4, pp. 15–26, 2009.